



# Effect of synthesis temperature on crystallinity, morphology and cell viability of nanostructured hydroxyapatite via wet chemical precipitation method

Effect of temperature on hydroxyapatite properties

AL. Rosa<sup>1</sup>; LR. Farias<sup>1</sup>; VP. Dias<sup>1</sup>; OB. Pacheco<sup>1</sup>; FDP. Morisso<sup>2</sup>; LF. Rodrigues Junior<sup>3</sup>; MR. Sagrillo<sup>3</sup>; A. Rossato<sup>3</sup>; LL. Santos<sup>4</sup>; TM. Volkmer<sup>1\*</sup>

\*Corresponding author: e-mail address: [tiagovolkmer@gmail.com](mailto:tiagovolkmer@gmail.com)

**Abstract:** Hydroxyapatite (HA) is the main natural mineral constituent of bones and is a good alternative for biomedical applications because it is osteoconductive, non-allergenic, and non-carcinogenic, which ensures high biocompatibility. A commonly used method for obtaining hydroxyapatite is the wet route, which is simple and low-cost, produces only water as a final residue, and provides HA with a crystallinity comparable to that of bone tissue, which favors its biocompatibility. Therefore, the objective of this work is to synthesize hydroxyapatite via the wet chemical precipitation method at different temperatures (4°C, 30°C, 50°C, or 70°C) to observe the influence of temperature on crystallinity, morphology, and cytotoxicity. The results of X-ray diffraction show that all syntheses resulted in pure hydroxyapatite, while increasing the temperature led to higher crystallinity (10.6% to 56.2%) and the crystal size was slightly affected. The increase in temperature changed the particle shape from irregular to needle-like. Cell viability was tested by PicoGreen® in VERO cells for samples at concentrations of 30 and 300 µg/mL, and the samples synthesized at 4°C, with lower crystallinity, caused less DNA damage to cells compared to the negative control.

**Keywords:** Calcium phosphate. Bioceramics. PicoGreen®. Scherrer's equation.

## Introduction

Over the years, the need for replacement of damaged bone tissues has been increasing, and it is in this context that ceramic biomaterials arise, among which hydroxyapatite (HA) stands out<sup>1</sup>. The crystal structure and chemical composition presented by hydroxyapatite are similar to the composition of human bones and teeth. It is a bioactive ceramic material that presents biocompatibility and promotes the formation of bonds with bone tissue<sup>2-4</sup>, as well as anticancer properties<sup>5</sup>. These factors have been crucial, justifying the numerous studies developed regarding its production and application in the biomedical field, particularly in the replacement of bone tissues<sup>3,5</sup>.

One of the factors that has the greatest influence on the biocompatibility of hydroxyapatite as a substitute for bone tissue in the human body is its crystallinity. Hydroxyapatites with lower crystallinity have a higher rate of protein adsorption as well as an increase in the rate of release of bioactive calcium and phosphorus. These results in an increase in cell adhesion, proliferation, and differentiation compared to hydroxyapatites with high crystallinity. The promising effect of low crystallinity hydroxyapatite is due to the fact that in a crystal structure with this characteristic, solubility in body fluids is facilitated, which increases its bioactivity<sup>5</sup>.

Among HA synthesis methods, the wet precipitation consists of preparing two solutions, one alkaline and one

acidic, where the acidic solution is slowly dripped into the alkaline solution, resulting in the precipitation step of HA. After this step, the filtration, drying, and thermal treatment of HA follow<sup>4</sup>. Some of the advantages presented by this HA obtaining technique are low reaction temperatures, control of chemical composition, and control of microstructural properties<sup>6</sup>. The morphology<sup>3,4</sup> and stoichiometry of the obtained material can be altered according to parameters such as reaction time, reaction temperature, concentration<sup>4</sup>, and "type/source" of reagents used<sup>3</sup>, as well as drying and thermal treatment conditions<sup>4</sup>.

Wet method synthesis temperature can alter some properties, such as crystallite size and degree of crystallinity, which may influence the biocompatibility of hydroxyapatite<sup>2,6</sup>. So HA will be synthesized at four different temperatures and the effect on the powder phases, morphology, crystallite size, crystallinity and biocompatibility will be analyzed.

## Materials and Methods

In the present study, hydroxyapatite powder was synthesized using the wet precipitation method. Hydroxyapatite nanoparticles were prepared by using 0.5M calcium hydroxide (Ca(OH)<sub>2</sub>) in an aqueous suspension that was temperature-controlled as required. Then, a 0.3M phosphoric acid solution was added at an addition rate of 2.5 mL/min to the calcium hydroxide suspension. The

<sup>1</sup> Pelotas Federal University.

<sup>2</sup> Feevale University.

<sup>3</sup> Franciscana University.

<sup>4</sup> Rio Grande do Sul Federal University.

Received 15 January 2022; Accepted 10 February 2022; Available online 11 February 2022.

 <https://doi.org/10.52466/ijamb.v5i1.110>

synthesis was carried out at four different temperatures, namely 4, 30, 50, and 70°C. The resulting solution was vigorously stirred for a period of 2 hours. The mixture was then filtered by vacuum filtration and dried at 100°C for 24 hours. Subsequently, the resulting white powder was macerated with a pestle and passed through a #200 mesh sieve before being separated for the following characterizations. In order to identify the present phases in the material synthesized at different temperatures, X-Ray diffractometer (D2 Phaser, Bruker) with a copper anode (CuK $\alpha$  radiation,  $\lambda=1.5406 \text{ \AA}$ ) with voltage and current values of 30 kV e 10 mA, respectively and the scan rate was 0,05064 degree/s. The (020) plane was used to calculate the crystallite size by Scherrer's equation<sup>7</sup>

Hydroxyapatite crystallinity (Xc) was calculated using equation 1<sup>8</sup>:

$$Xc = 1 - \left( V_{112/300} / I_{300} \right) \quad (\text{eq. 1})$$

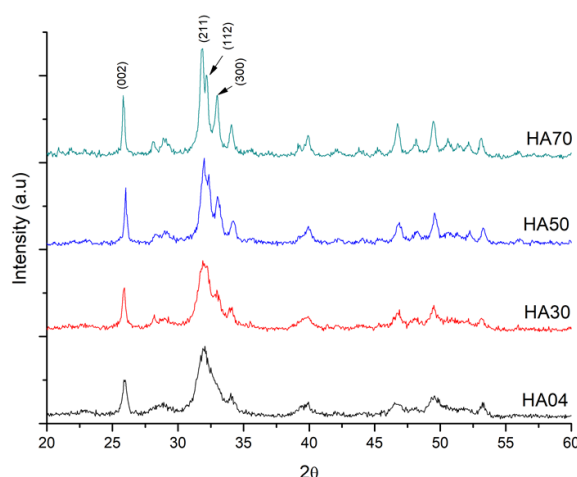
Where Xc is the crystallinity of the HA,  $V_{112/300}$  is the intensity of the valley between the diffraction peaks corresponding to the (112) and (300) planes, and  $I_{300}$  is the intensity of the peak corresponding to the (300) plane. The specific surface area was determined by nitrogen adsorption-desorption of Nitrogen (Quantachrome Instruments, NOVA 2200e) at 200 °C for 12 /h. To identify the functional groups present in the samples, Fourier transform infrared spectroscopy-attenuated total reflectance (FTIR-ATR) spectra were recorded (Perking Elmer, Spectrum Two). Powder morphology was verified by SEM (JOEL, JSM-6510LV). The thermal behavior of the materials was investigated using the technique of thermogravimetric analysis, using a Shimadzu TGA-51H equipment. A prospective in vitro study was conducted, in which a commercial cell line, adult monkey renal epithelial cells (VERO cell line), was used as an experimental model to investigate potential cytotoxic effects. After thawing, this cell line was maintained in polystyrene bottles (TPP) in culture medium containing 10% fetal bovine serum (Invitrogen), inactivated at 56°C for 1 hour, 100  $\mu$ /mL of penicillin (Invitrogen), and 100  $\mu$ /mL of streptomycin (Invitrogen), at 37°C in a humid atmosphere containing 5% CO<sub>2</sub>. Weekly passages were performed in a laminar flow hood, so that each bottle received 5 mL of medium with a fixed number of cells at the time of passage ( $2.0 \times 10^5$  cells/mL). The volume, along with the above number of cells, was transferred to a new bottle with fresh medium. After obtaining satisfactory confluence for the experimental assays, the cells were seeded in 24-well plates. After the treatments, the plates were incubated in a CO<sub>2</sub> incubator at 37°C for 24 hours. The experiments were performed in triplicate. The evaluation of the cytotoxic

effect of the structures was tested through the DNA PicoGreen® assay. To complement the determination of cell viability, a fluorimetric assay was conducted to quantify free DNA in the medium using the PicoGreen® reagent from Invitrogen (Life Technologies), which is a fluorescent dye that binds to double-stranded DNA. This procedure was performed in the culture medium where the cells are treated to determine the presence of double-stranded DNA in this medium due to possible cell rupture and cell death. The dye was added to the sample in a 96-well dark Elisa plate, with incubation for 5 minutes and fluorescence reading in the spectrofluorometer at 480 nm excitation and 520 nm emission<sup>9</sup>.

## Results and discussion

The X-ray diffraction (XRD) patterns of synthesized HA powders are displayed in Figure 1.

**Figure 1**– X-ray diffraction patterns of samples synthesized at different temperatures.



The X-ray diffraction peaks at  $2\theta = 25.8, 31.9, 32.2$  and  $32.9$  correspond to the standard crystallographic file of pure hydroxyapatite (PDF - 009-00432). There were no undesirable phases such as  $\beta$ -TCP and CaO detected in any of the synthesized powders. The crystalline planes shown in the samples are (002), (211), (112) and (300)<sup>5,8</sup>. It can be observed that the increase of synthesis temperature, lead to an increase in peaks intensity. This growth occurred especially on the (002) peak, which indicates the growth of HA crystals along C-axis<sup>7</sup>. Table 1. shows crystallite size obtained by Scherer's equation, crystallinity degree calculated using equation 1 and specific surface area obtained by BET.

The crystallinity percentage of hydroxyapatite samples increased with synthesis temperature from 10.6 to 56.2, while the crystallite size increased from 27.4 to 42.2 nm. On the other hand, the specific surface area decreased from 90.9 to 50.1 m<sup>2</sup>/g. György *et al*<sup>10</sup>, relate the peak broadening effect of XRD patterns from

hydroxyapatite synthesized at low temperatures to either smaller crystallinity and crystallite size. The crystal size of hydroxyapatite (HA) changes with temperature during synthesis. During the early stages of particle formation, nucleation occurs, where small HA particles are formed. As the reaction progresses, these small particles begin to grow in size with the incorporation of additional calcium and phosphate ions from the solution<sup>15,16</sup>. Conversely, there was a decrease of the specific surface area measured by BET as a function of the increase in precipitation temperature, the same tendency was found by Lazic *et al.*<sup>11</sup> that synthesized HA in the temperature range of 22 – 95°C and obtained a specific surface area in the range of 58–23 m<sup>2</sup>/g. The specific surface area of hydroxyapatite is an important factor since it can affect protein adsorption<sup>12</sup>. Figure 2 shows the FTIR spectra for the four synthesized samples.

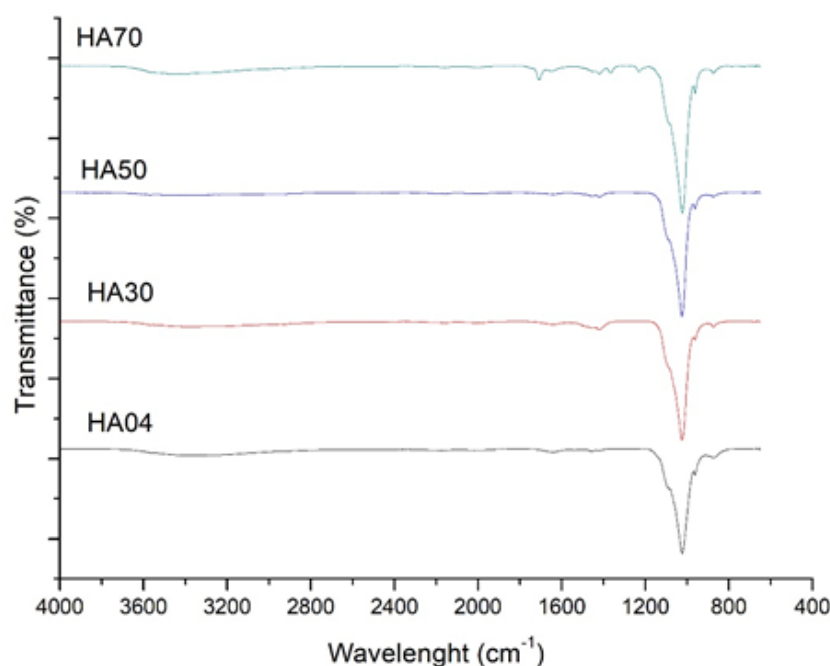
It is possible to visualize hydroxyapatite characteristic band peaks for all samples. The broad band around 3400 cm<sup>-1</sup>, can be attributed to hydroxyl group<sup>13–15</sup>. With the

increase in synthesis temperature, there was an increment in the observed band at 1642 cm<sup>-1</sup> which corresponds to the bending mode of H–O–H in water, indicating the presence of trace amounts of water in the synthesized powders<sup>2</sup>. The increase can also be observed in the peaks between 1400–1500 cm<sup>-1</sup>, which correspond to the CO<sub>3</sub><sup>2-</sup> vibrational peaks. These peaks replace some of the phosphate groups in the hydroxyapatite from natural<sup>14,16</sup>. According to Dey *et al.*<sup>2</sup>, those CO<sub>3</sub><sup>2-</sup> bands can appear in hydroxyapatites obtained by wet synthesis, due to the dissolution of atmospheric CO<sub>2</sub> in the reaction. Higher synthesis temperatures can facilitate CO<sub>2</sub> diffusion. A pronounced band at approximately 1024 cm<sup>-1</sup> and a smaller peak at 965 cm<sup>-1</sup> correspond to asymmetric (P–O) stretching vibration PO<sub>4</sub><sup>3-</sup>, while the presence of HPO<sub>4</sub><sup>2-</sup> in these powders is indicated by the 876 cm<sup>-1</sup> transmission band<sup>13</sup>. Figure 3 shows the thermal analysis of HA investigated by thermal gravimetric analysis (TGA).

**Table 1** – Crystallinity, crystallite size and specific surface area of hydroxyapatite synthesized at different temperatures.

Sample	% Crystallinity	Crystallite size (nm)	Specific Surface Area (m <sup>2</sup> /g)
HA04	10.6	27.4	90.9
HA30	16.4	33.5	78.2
HA50	41.5	34.4	59.9
HA70	56.2	42.2	50.1

**Figure 2** – FTIR spectrum of hydroxyapatite synthesized at different temperatures.



It is possible to notice a sharp drop from 30°C to around 200°C related to the elimination of adsorbed water<sup>10,17</sup>. The small mass decrease in the region between 200 and 650°C can be attributed to the removal of interstitial water<sup>17</sup>. For the hydroxyapatite synthesized at 4°C there was a small drop in the mass related to the conversion of the hydroxyapatite into  $\beta$ -tricalcium phosphate ( $\beta$ -TCP)<sup>10</sup>. Precipitation temperature has shown a significant effect on HA morphology, as can be seen in figure 4.

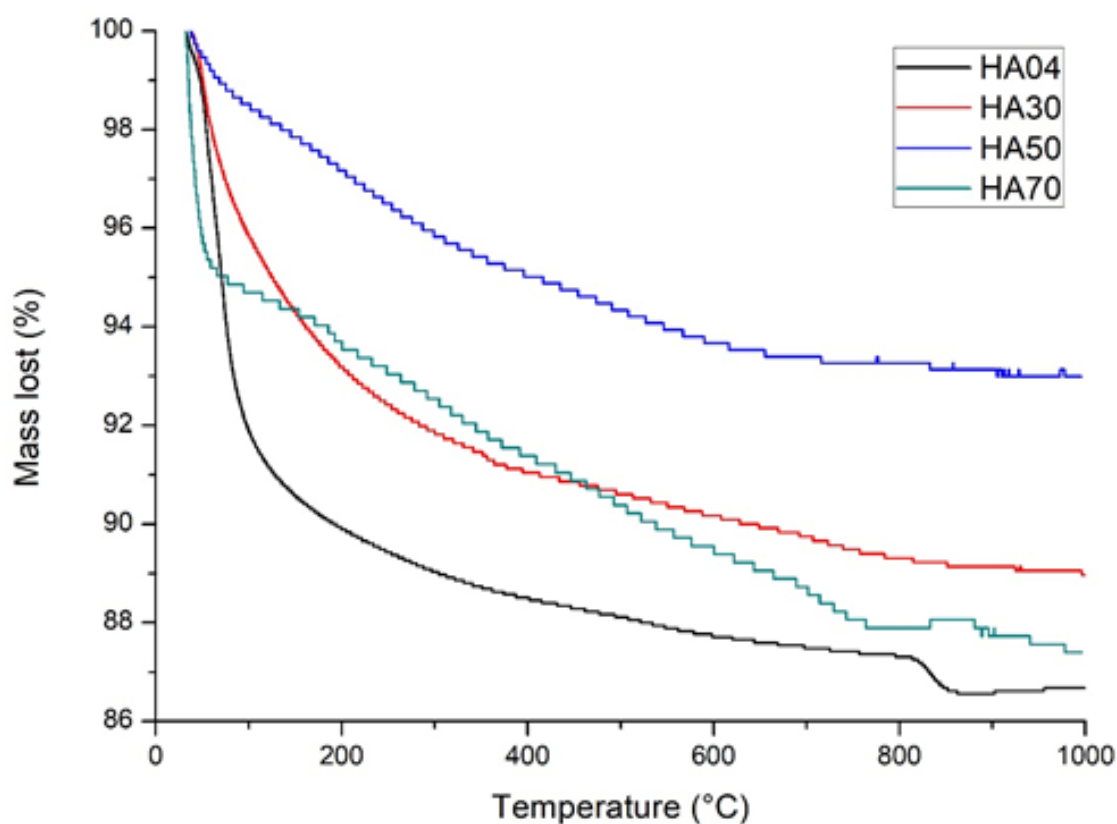
The effectiveness of nucleus growth and development plays a vital role in determining the crystalline structure of materials produced through the wet precipitation process, which functions via the nucleation-growth mechanism<sup>4</sup>, this can be attributed to the size-dependent solubility of nanoparticles (NPs), where smaller particles exhibit higher solubility and surface energy, facilitating the dissolution and growth of larger particles<sup>18</sup>.

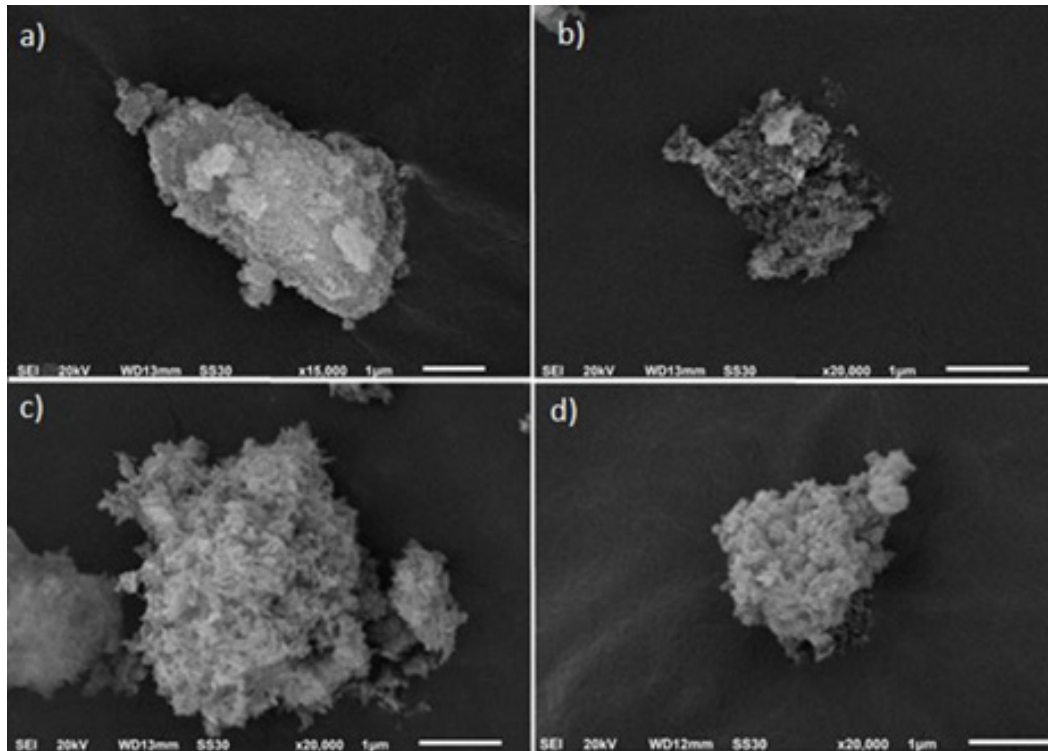
Further research has indicated that the synthesis of hydroxyapatite at low temperatures results in crystals with irregular morphology, a lower specific surface area, and a greater tendency to agglomerate<sup>4</sup>. At a temperature of 4°C, the particles tend to aggregate, making it

challenging to discern their morphology, indicating that there is insufficient driving force for crystal growth at low temperatures<sup>10</sup>. As the reaction temperature is raised, crystal growth is observed, consistent with the typical needle-like morphology of hydroxyapatite observed in X-ray Diffraction data<sup>10,19</sup>. To evaluate cell viability, a fluorometric test for quantifying free DNA was conducted. The DNA-PicoGreen<sup>®</sup> assay involves using a fluorescent dye that binds to double-stranded DNA in the medium, allowing for the detection of possible cell disruption and cell death<sup>20</sup>. To verify cell damage, two different concentrations of hydroxyapatite (30 and 300  $\mu\text{g}/\text{mL}$ ) for each synthesis temperature. Figure 5. shows the results obtained from the DNA-PicoGreen<sup>®</sup> assay.

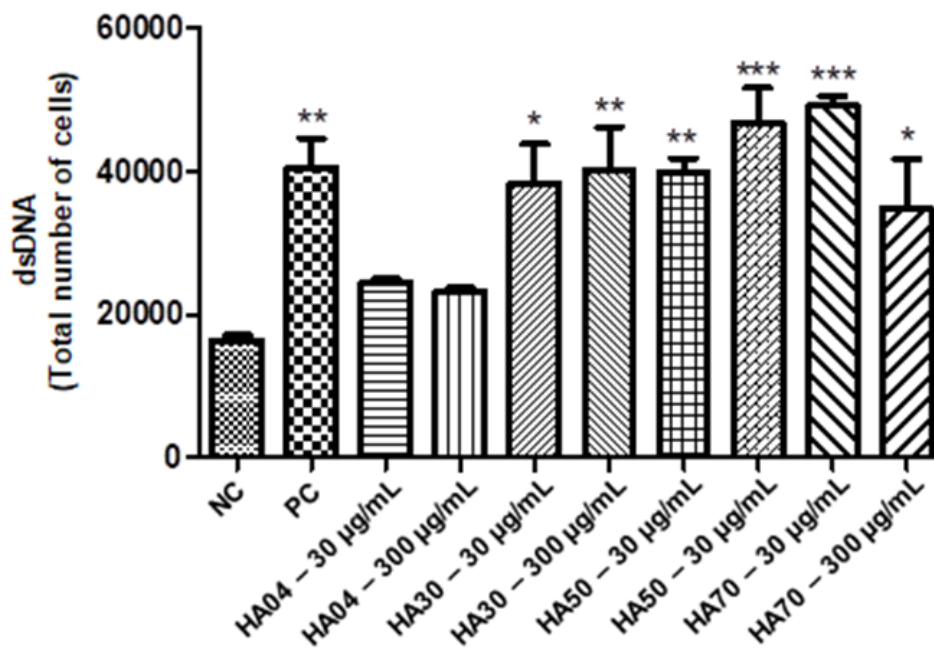
The results showed no significant damage to the double strain DNA in HA04 sample for both concentrations. However, for other temperatures of synthesis the damage to the DNA was close to the positive control. According to Zhao<sup>20</sup>, hydroxyapatite cytotoxicity depends on nanoparticle shape and that needle-like particles are more toxic than other shapes.

**Figure 3** – TGA analysis of hydroxyapatite synthesized at different temperatures.



**Figure 4** – SEM micrographs of hydroxyapatite

**Figure 5** – Evaluation of the presence of double-stranded DNA using the PicoGreen® assay. NC (control negative); PC (control positive); HA04, HA30, HA50 and HA70 (30 and 300 µg/mL). Data are expressed as mean ± standard deviation (SD). Analyses were followed by one-way ANOVA, followed by Dunnett's post hoc test. Values with  $p < 0.05$  were considered statistically significant, where \*  $p < 0.05$ , \*\*  $p < 0.01$  and \*\*\*  $p < 0.001$ .



## Conclusions

The wet synthesis of hydroxyapatite was carried out at temperatures of 4, 30, 50, and 70°C. X-ray diffraction revealed that HA was the only phase present in the synthesized powders. There was an increase in crystallinity and crystallite size with increasing temperature, resulting in a hexagonal crystalline phase. Additionally, an increase in particle size and a decrease in surface area were observed by BET analysis. The irregular shape of nanoparticles synthesized at low temperatures was confirmed by SEM analysis also, there was a transition to needle-like structures with increasing temperature, which is characteristic of HA with elongation along the c-axis. The FTIR bands were characteristic of pure HA, and the mass losses observed by thermogravimetry were consistent with those of HA samples. In the cell viability test using PicoGreen®, lower toxicity was observed at 4°C compared to higher temperatures.

## References

- [1]. Avanzi IR, Parisi JR, Souza A, Cruz MA, Martignago CCS, Ribeiro DA, et al. 3D-printed hydroxyapatite scaffolds for bone tissue engineering: A systematic review in experimental animal studies. Vol. 111, Journal of Biomedical Materials Research – Part B Applied Biomaterials. John Wiley and Sons Inc; 2023. p. 203–19.
- [2]. Dey S, Das M, Balla VK. Effect of hydroxyapatite particle size, morphology and crystallinity on proliferation of colon cancer HCT116 cells. Materials Science and Engineering C. 39(1):336–9 (2014).
- [3]. DileepKumar VG, Sridhar MS, Aramwit P, Krut'ko VK, Muskaya ON, Glazov IE, et al. A review on the synthesis and properties of hydroxyapatite for biomedical applications. Vol. 33, Journal of Biomaterials Science, Polymer Edition. Taylor and Francis Ltd.; 2022. p. 229–61.
- [4]. Méndez-Lozano N, Apátiga-Castro M, Soto KM, Manzano-Ramírez A, Zamora-Antuñano M, González-Gutiérrez C. Effect of temperature on crystallite size of hydroxyapatite powders obtained by wet precipitation process. Journal of Saudi Chemical Society. 26(4) (2022).
- [5]. Zhang L, Lu T, He F, Zhang W, Yuan X, Wang X, et al. Physicochemical and cytological properties of poorly crystalline calcium-deficient hydroxyapatite with different Ca/P ratios. Ceram Int. 48(17):24765–76 (2022).
- [6]. Yelten A, Yilmaz S. Various Parameters Affecting the Synthesis of the Hydroxyapatite Powders by the Wet Chemical Precipitation Technique. In: Materials Today: Proceedings. Elsevier Ltd; 2016. p. 2869–76.
- [7]. Lin TJ, Heinz H. Accurate Force Field Parameters and pH Resolved Surface Models for Hydroxyapatite to Understand Structure, Mechanics, Hydration, and Biological Interfaces. Journal of Physical Chemistry C. 120(9):4975–92 (2016).
- [8]. Han JK, Song HY, Saito F, Lee BT. Synthesis of high purity nano-sized hydroxyapatite powder by microwave-hydrothermal method. Mater Chem Phys. 99(2–3):235–9 (2006).
- [9]. Sagrillo MR, Garcia LFM, De Souza Filho OC, Duarte MMMF, Ribeiro EE, Cadoná FC, et al. Tucumã fruit extracts (*Astrocaryum aculeatum* Meyer) decrease cytotoxic effects of hydrogen peroxide on human lymphocytes. Food Chem. 173:741–8 (2015).
- [10]. György S, Károly Z, Fazekas P, Németh P, Bódis E, Menyhárd A, et al. Effect of the reaction temperature on the morphology of nanosized HAp. J Therm Anal Calorim. 138(1):145–51 (2019).
- [11]. Lazic S, Zec S, Miljevic N, Milonjic S. The effect of temperature on the properties of hydroxyapatite precipitated from calcium hydroxide and phosphoric acid.
- [12]. Wu F, Lin DDW, Chang JH, Fischbach C, Estroff LA, Gourdon D. Effect of the materials properties of hydroxyapatite nanoparticles on fibronectin deposition and conformation. Cryst Growth Des. 15(5):2452–60 (2015).
- [13]. Bouropoulos N, Stampoulakis A, Mouzakis DE. Dynamic mechanical properties of calcium alginate-hydroxyapatite nanocomposite hydrogels. Sci Adv Mater. 2(2):239–42 (2010).
- [14]. Chandrasekaran A. Synthesis and characterization of nano-hydroxyapatite (n-HAP) using the wet chemical technique Zirconia Reinforced Polymer nano composite International Journal of Physical Sciences. (2013).
- [15]. Sahana H, Khajuria DK, Razdan R, Mahapatra DR, Bhat MR, Suresh S, et al. Improvement in bone properties by using risedronate adsorbed hydroxyapatite novel nanoparticle based formulation in a rat model of osteoporosis. J Biomed Nanotechnol. 9(2):193–201 (2013).
- [16]. Gheisari H, Karamian E, Abdellahi M. A novel hydroxyapatite –Hardystonite nanocomposite ceramic. Ceram Int. 41(4):5967–75 (2015).
- [17]. Lazic S, Zec S, Miljevic N, Milonjic S. The effect of temperature on the properties of hydroxyapatite precipitated from calcium hydroxide and phosphoric acid.

- [18]. Thanh NTK, Maclean N, Mahiddine S. Mechanisms of nucleation and growth of nanoparticles in solution. Vol. 114, Chemical Reviews. American Chemical Society; 2014. p. 7610–30.
- [19]. Sossa PAF, Giraldo BS, Garcia BCG, Parra ER, Arango PJA. Comparative study between natural and synthetic hydroxyapatite: Structural, morphological and bioactivity properties. *Revista Materia*. 23(4) (2018).
- [20]. Zhao X, Ng S, Heng BC, Guo J, Ma L, Tan TTY, et al. Cytotoxicity of hydroxyapatite nanoparticles is shape and cell dependent. *Arch Toxicol*. 87(6):1037–52 (2013).